A new high performance field reversed configuration operating regime in the C-2 device[a)]

M. Tuszewski,[1,b)] A. Smirnov,[1] M. C. Thompson,[1] T. Akhmetov,[2] A. Ivanov,[2] R. Voskoboynikov,[2] D. Barnes,[1] M. W. Binderbauer,[1] R. Brown,[1] D. Q. Bui,[1] R. Clary,[1] K. D. Conroy,[1] B. H. Deng,[1] S. A. Dettrick,[1] J. D. Douglass,[1] E. Garate,[1] F. J. Glass,[1] H. Gota,[1] H.Y. Guo,[1] D. Gupta,[1] S. Gupta,[1] J. S. Kinley,[1] K. Knapp,[1] S. Korepanov,[1] A. Longman,[1] M. Hollins,[1] X. L. Li,[1] Y. Luo,[1] R. Mendoza,[1] Y. Mok,[1] A. Necas,[1] S. Primavera,[1] E. Ruskov,[1] L. Schmitz,[3] J. H. Schroeder,[1] L. Sevier,[1] A. Sibley,[1] Y. Song,[1] X. Sun,[1] E. Trask,[1] A. D. Van Drie,[1] J. K. Walters,[1] M. D. Wyman,[1] and the TAE Team
[1]*Tri Alpha Energy, Inc., P.O. Box 7010, Rancho Santa Margarita, California 92688, USA*
[2]*Budker Institute of Nuclear Physics, Novosibirsk 630090, Russia*
[3]*Department of Physics and Astronomy, UCLA, Los Angeles, California 90095-1547, USA*

(Received 13 December 2011; accepted 26 February 2012; published online 28 March 2012)

Large field reversed configurations (FRCs) are produced in the C-2 device by combining dynamic formation and merging processes. The good confinement of these FRCs must be further improved to achieve sustainment with neutral beam (NB) injection and pellet fuelling. A plasma gun is installed at one end of the C-2 device to attempt electric field control of the FRC edge layer. The gun inward radial electric field counters the usual FRC spin-up and mitigates the $n = 2$ rotational instability without applying quadrupole magnetic fields. Better plasma centering is also obtained, presumably from line-tying to the gun electrodes. The combined effects of the plasma gun and of neutral beam injection lead to the high performance FRC operating regime, with FRC lifetimes up to 3 ms and with FRC confinement times improved by factors 2 to 4. © *2012 American Institute of Physics*. [http://dx.doi.org/10.1063/1.3694677]

I. INTRODUCTION

The field reversed configuration (FRC) is a prolate compact toroid formed with poloidal magnetic fields.[1,2] The FRC continues to be explored experimentally and theoretically, because it offers a high potential for a fusion reactor, including very high-beta, simple geometry, natural divertor, and ease of translation. The FRC could lead to an economic fusion reactor with high fusion power density, possibly using aneutronic fuels such as D-He^3 and p-B^{11}.

Large FRCs are produced in the C-2 device by combining dynamic formation and merging processes.[3,4] Two compact toroids, formed ($t = 0$) by a variant of the field reversed theta-pinch method, are translated supersonically into a central stainless-steel confinement vessel where they collide ($t \sim 30\ \mu s$) and progressively merge into a long-lived (~1 ms) FRC. An FRC equilibrium in the C-2 device is shown in Fig. 1, as calculated from the Lamy-Ridge code.[5] Field line contours are traced, and plasma densities are indicated with colors.

Typical C-2 equilibrium FRC parameters are ($t = 0.3$ ms): separatrix radius $r_s \sim 0.4$ m, separatrix length $L_s \sim 3$ m, external magnetic field $B_e \sim 1$ kG, average density $n \sim 4 \times 10^{19}$ m^{-3}, deuterium ion temperature $T_i \sim 0.5$ keV, and electron temperature $T_e \sim 0.2$ keV. The FRC lifetimes are ~1 ms. During the decay, the FRC separatrix shrinks radially and axially, and the plasma temperatures gradually decrease.

The main goal of the C-2 experiment is to demonstrate FRC sustainment with neutral beam (NB) injection for heating and current drive and with pellet injection for particle refueling. The C-2 20 keV hydrogen NBs are injected tangentially to the FRC current direction (co-injection), with an impact parameter of 0.2 m. The FRC parameters listed above are suitable for NB capture (Monte-Carlo simulations indicate that shine-through and first orbit losses less than 10%) and for fast ion confinement (slowing down time ~ FRC lifetime). The 20 keV fast ions have betatron orbits with large excursions outside the FRC separatrix (typical outer turning radii are ~0.55 m.).

The confinement properties of the C-2 FRCs are good,[3,4] comparable or exceeding those of past FRCs.[1,2] However, further improvement in the FRC confinement is desirable. The global power losses are about 10 MW midway ($t \sim 0.5$ ms) through the FRC lifetime. Hence, they exceed substantially the available NB input power to the FRC. Accordingly, present C-2 research seeks new ways to improve FRC confinement, while attempting to build up a significant fast ion population.

Rotational stability also remains a concern for C-2 FRCs, as will be detailed in Sec. II. During the last year, new experimental techniques have substantially improved the confinement and stability of C-2 FRCs. A plasma gun introduced at one end of the C-2 device is key, together with NB injection, to obtain much improved FRC data. This paper reports on these new results, referred to as the high performance FRC (HPF) operating regime.

The present paper is organized as follows. Section II details FRC rotational stability and how it can impact NB fast ion confinement. Section III describes the C-2 end plasma

[a)]Paper YI3 6, Bull. Am. Phys. Soc. **56**, 362 (2011).
[b)]Invited speaker.

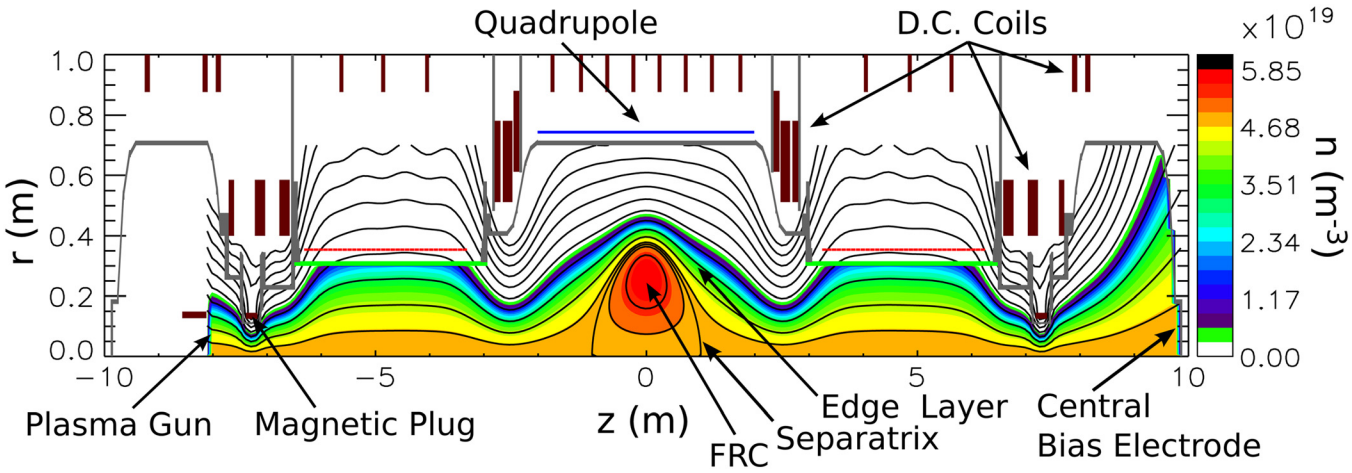

FIG. 1. Sketch of an FRC equilibrium inside the modified C-2 device.

gun and its main beneficial attributes. An attempt is made to dissect the new HPF operating regime in Sec. IV, one component at a time. The data are discussed in Sec. III and the results are summarized in Sec. VI.

II. FRC ROTATIONAL STABILITY

The C-2 FRCs are grossly stable, presumably because of kinetic effects.[3,4] These FRCs have $s \sim 1$ (s is the ratio of the FRC minor radius to the average internal ion gyroradius), $S^* \sim 8$ (S^* is the ratio of the FRC separatrix radius to the average collisionless ion skin-depth), and separatrix elongations $E \sim 4$. With $S^*/E \sim 2$, the C-2 FRCs remain well inside the kinetically tilt-stable FRC parameter space.[2]

All FRCs develop an azimuthal rotation in the ion diamagnetic direction. The FRC spin-up is clearly observed in the C-2 device with various magnetic probe and bolometer arrays. The origin of the rotation remains to be clarified, but end-shorting of the radial electric field on open field lines and particle loss from inside the FRC separatrix are leading explanations.[1,2,6]

The FRC azimuthal ion rotation consists of electric and diamagnetic components, as can be seen from the equilibrium ion momentum equation

$$ne(\mathbf{E} + \mathbf{v}_i \times \mathbf{B}) - \nabla p_i = 0. \quad (1)$$

In the FRC midplane, to lowest order, the electric field and the ion pressure gradient are radial, the magnetic field is axial, and the ion velocity is azimuthal. The radial electric field can be obtained from the radial component of Eq. (1) as

$$E_r = r\Omega^* B(\alpha - 1), \quad (2)$$

where $\alpha = \Omega/\Omega^*$ is a normalized ion rotation parameter, $\Omega = v_{i\theta}/r$ is the ion angular rotation frequency, and $\Omega^* = (dp_i/dr)/(enrB)$ is the ion diamagnetic frequency. Both B and Ω^* are chosen to be positive quantities. Rotation is positive in the ion diamagnetic direction ($\alpha > 0$). One observes from Eq. (2) that E_r is positive (outward) for $\alpha > 1$ and negative (inward) for $\alpha < 1$.

Rotational instabilities develop soon after the FRC starts to rotate. The $n = 1$ "wobble" grows for small α values. Mirnov probes reveal wobble motion for C-2 FRCs with $\alpha \sim 0.1$, consistent with similar past measurements in the FRX-C/LSM device.[7] An $n = 2$ elliptical mode develops for $\alpha > 1 - 1.5$.[1,2] Without stabilization, the $n = 2$ mode grows quickly to large amplitude and is destructive with a dielectric first wall (*in-situ* theta-pinches).

The $n = 2$ mode is clearly observed for C-2 FRCs at $t > 0.2$ ms, with multi-chord side-on interferometry and bolometer arrays.[3,4] It saturates at large amplitude in the C-2 confinement vessel, presumably because of wall stabilization. The significant elliptical plasma deformations somewhat compromise the FRC plasma confinement. Recent data and calculations, to be published elsewhere, suggest that the elliptical deformations can also affect significantly the NB fast ion confinement.

The $n = 2$ mode can be stabilized with external multipole magnetic fields, a technique used in most FRC experiments following PIACE results.[8] Quadrupole magnetic fields are used in the C-2 device to permit side-on NB access. Typical C-2 operation includes 15 kA in each quadrupole bar. This current produces a vacuum magnetic field of about 90 G at $r = 0.4$ m, which is enough to stabilize the $n = 2$ mode through most of the FRC lifetime, as the separatrix shrinks radially. This reference quadrupole current is abbreviated as $q = 1$ later in this paper.

Quadrupole stabilization is effective in preventing the FRC elliptical deformation, but it has some negative aspects. The combined mirror and quadrupole magnetic fields fan in and out the edge layer field lines and compromise communication to the ends of the C-2 device. Lower FRC temperatures are observed in the C-2 device for $q = 1$.

The applied quadrupoles break azimuthal symmetry (canonical angular momentum), which can deteriorate mirror plasma confinement.[9] The quadrupoles can also cause rapid stochastic diffusion of the NB fast ion orbits to the wall.[10,11] Similar fast ion losses can occur for FRCs sustained with rotating (dipole) magnetic fields.[12]

FRC rotational stability is, therefore, a serious concern for C-2 experimental plans. Without quadrupoles, the FRC is not axisymmetric as its cross-section deforms into an ellipse. With quadrupoles, the applied magnetic field is not

axisymmetric. NB fast ion confinement deteriorates in both cases. Hence, a new axisymmetric technique to control FRC rotational instabilities is highly desirable.

Equation (2) suggests that one could obtain $\alpha < 1$ by imposing an inward radial electric field ($E_r < 0$) near the separatrix. The $n = 2$ mode growth may be suppressed, since it occurs for $\alpha > 1$. Various experimental techniques have been tried on the C-2 device to control the radial electric field in the FRC edge layer, with various degree of success. We focus here on the end plasma gun data, because it proves so far to be the most successful technique for E_r control.

III. END PLASMA GUN

A plasma gun and two magnetic field end plugs are added to the C-2 device, as sketched in Fig. 1. The plasma gun is located on axis at $z = -8$ m, inside the South divertor. The two end plugs (up to 2 T pulsed magnetic field) are located at $z = \pm 7.3$ m, between the formation regions and the divertors. The plasma gun and the end plugs have many potential benefits, such as improved FRC formation, edge layer confinement, particle refueling, stability through linetying to the gun, neutral gas control, radial electric field control of the FRC rotation, and creation of E×B velocity shear. Some of these benefits require a cold and dense plasma stream, while others require a hot tenuous plasma stream.

The AMBAL plasma gun is capable to produce either hot or cold plasmas.[13,14] The C-2 AMBAL plasma gun, obtained from the Budker Institute of Nuclear Physics, is sketched in Fig. 2. An annular (0.11 m inner diameter and 0.13 m outer diameter) plasma stream ($\sim 10^{22}$ D/s for $\sim$6 ms) is created with two gas valves and an anode to cathode voltage drop $\sim$0.5 kV. The gun arc current is $\sim$10 kA. The gun magnet provides an axial magnetic field $\sim$0.5 T.

For all data in this paper, the gun produces a hot ($T_e \sim 30 - 50$ eV and $T_i \sim 100$ eV) tenuous ($<10^{19}$ m^{-3}) plasma stream. These plasma parameters are estimated from diamagnetism just in front of the gun ($z \sim -8$ m) and in the formation quartz tube ($z \sim -6$ m) and from Langmuir probes and microwave interferometry ($z \sim -7$ m).

The gun also creates an inward electric field in the plasma stream. The radial profiles of probe floating potential

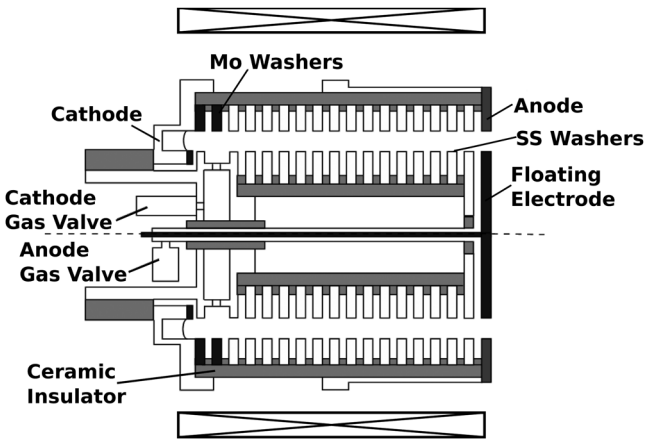

FIG. 2. The AMBAL plasma gun.

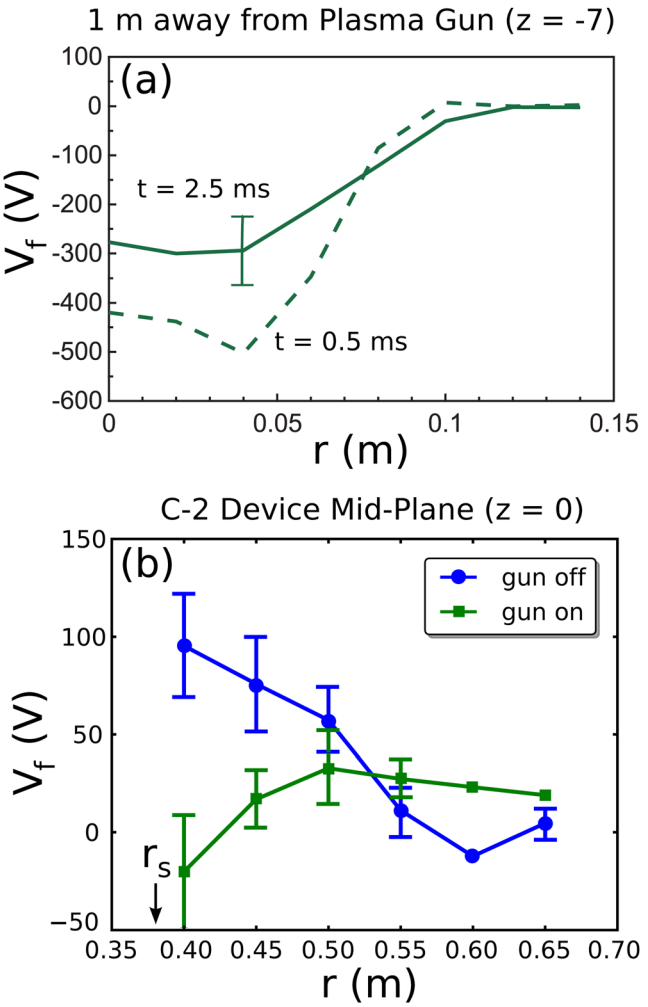

FIG. 3. Floating plasma potentials measured at (a) $z = -7$ m and (b) $z = 0$.

are shown in Fig. 3 at (a) $z = -7$ m for the gun alone and (b) in the FRC edge layer at $z = 0$ and at $t = 0.3$ ms. These triple probe data are acquired shot by shot, and typical standard deviations are indicated. Fig. 3(b) suggests that the radial electric field of the FRC edge layer is inward with the plasma

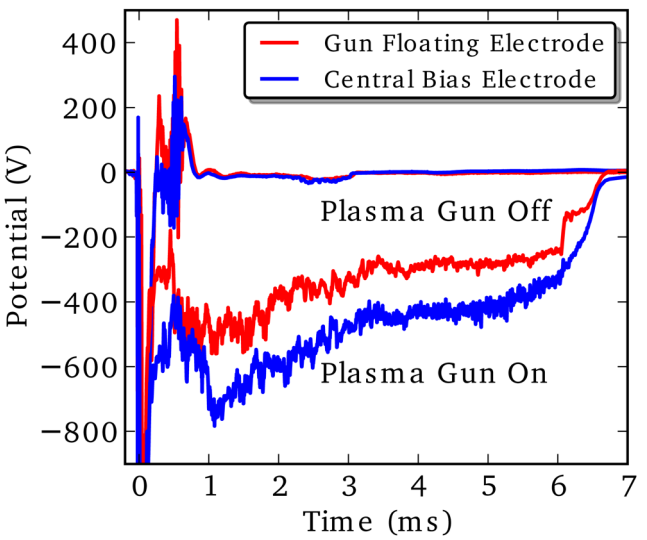

FIG. 4. Floating potentials of the gun front electrode and of the central end bias electrode, measured as functions of time.

gun and outward without it. These trends are only qualitative, because floating rather than plasma potentials are shown in Fig. 3. Probe measurements become increasingly difficult close to the FRC separatrix, and no data are available for $r < 0.4$ m.

The gun establishes a good electric communication along field lines through the entire C-2 device, as illustrated in Fig. 4. The potential of a floating electrode located on axis at $z \sim 10$ m (lower trace of plasma gun on state) tracks the potential of the gun floating electrode at $z = -8$ m (upper trace of plasma gun on state) for the 6 ms duration of the plasma stream. The potentials are around –0.5 kV, consistent with those measured in Fig. 3(a).

The plasma gun inward electric field counters the usual FRC spin-up and stabilizes the $n = 2$ rotational mode, as illustrated in Fig. 5. Side-on CO_2 interferometry[15] data at $z = 0$ are compared, (a) without the plasma gun and (b) with the plasma gun. These data are taken without NB injection after FRC formation and without quadrupoles ($q = 0$). The discharge in Fig. 5(a) shows easily recognizable $n = 2$ mode signatures[1,16] between 0.3 and 0.8 ms. The FRC elliptical deformation saturates, with a ratio of major to minor axes ~2, as estimated from interferometry maximum to minimum amplitudes[16] and from bolometer array reconstruction. The discharge in Fig. 5(b) shows no $n = 2$ oscillations up to about 0.9 ms (the FRC disrupts around that time).

The slow oscillation in Fig. 5(b) between 0.4 and 0.8 ms is an $n = 1$ wobble. Mirnov probes and bolometer arrays indicate that this $n = 1$ mode has a long wavelength (similar displacement along the FRC length) and rotates in the electron diamagnetic direction with a relatively small amplitude. This is illustrated in Fig. 6 with two C-2 discharges (a) without and (b) with the plasma gun. No quadrupoles ($q = 0$) are used in both cases. The trajectory of the FRC center is plotted as function of time, as estimated from two orthogonal bolometer arrays. Without the plasma gun, the $n = 1$ mode rotates first in the ion diamagnetic direction (red trace), before reversing in the electron diamagnetic direction (blue trace). The mode amplitude increases with time. With the plasma gun, the mode rotates in the electron diamagnetic direction (blue trace) at all times, with a relatively small (5 to 10 cm) amplitude.

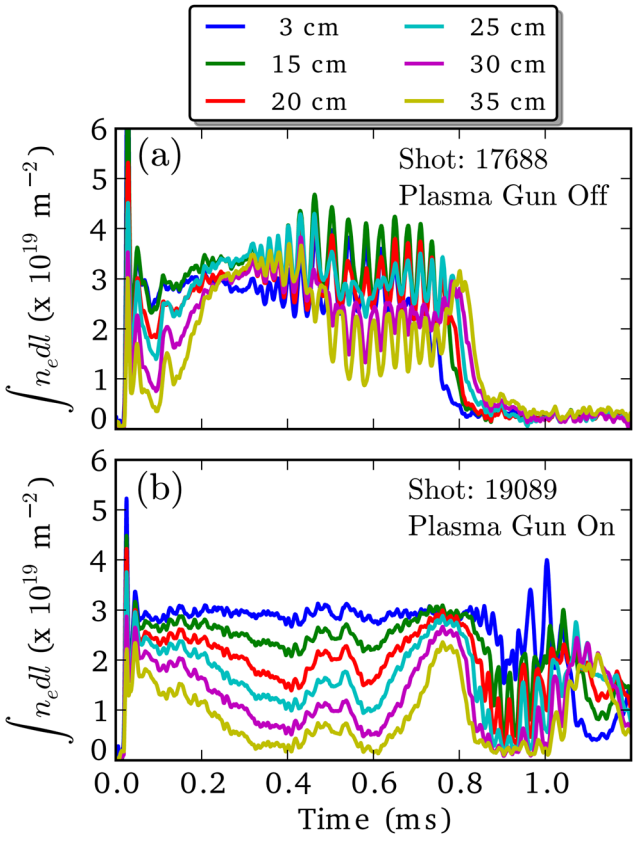

FIG. 5. Line-integrated densities of two C-2 discharges (a) without plasma gun and (b) with plasma gun.

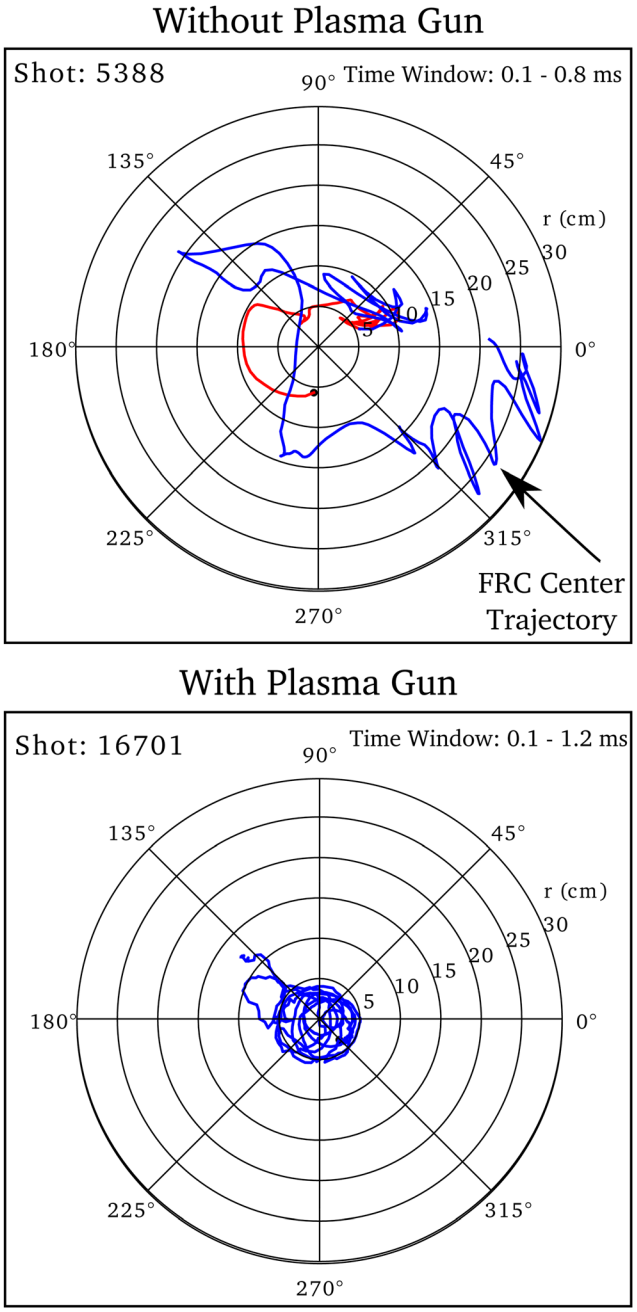

FIG. 6. Trajectories of the FRC center measured as functions of time (a) without plasma gun and (b) with plasma gun. The black dots indicate the starting point. Without the plasma gun, the FRC briefly moves in the ion diamagnetic direction before reversing and moving in the electron diamagnetic direction. With the plasma gun, motion is always in the electron diamagnetic direction.

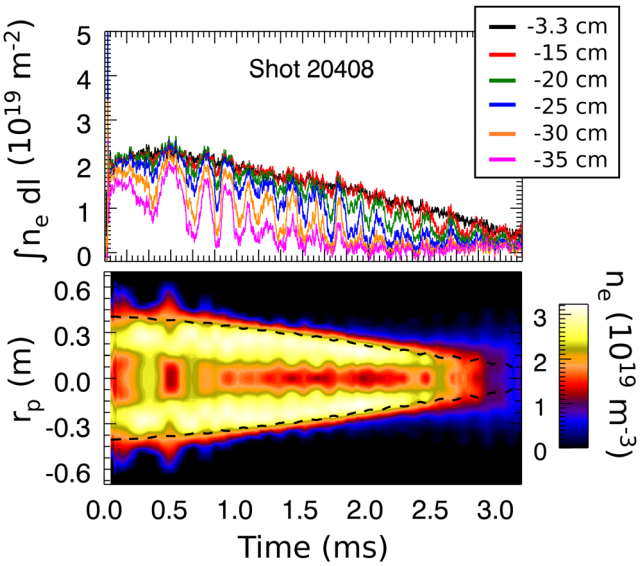

FIG. 7. A long-lived HPF discharge time history of (a) line-integrated densities and (b) Abel-inverted density profiles.

IV. THE HIGH PERFORMANCE FRC REGIME

The plasma gun yields control of the FRC rotational instabilities without using external multipoles. Hence, NBs are injected into near-axisymmetric FRC discharges. These discharges show much improved stability and confinement properties, from the combined effects of plasma gun and NB injection. Such conditions constitute the HPF operating regime.

An example of HPF data is shown in Fig. 7. Side-on interferometry data at $z = 0$ are shown as functions of time, with (a) 6 chords of line-integrated density and (b) Abel-inverted density profiles, assuming axisymmetry around the FRC center position. The latter is estimated from bolometer arrays, as in Fig. 6. The FRC density profiles in Fig. 7 are hollow up to at least 2.5 ms. The line-integrated densities become too low to resolve the profiles at late times. The dashed lines in Fig. 7(b) are the midplane excluded flux radii, $r\Delta\phi$, which approximate the separatrix radii.[1] There is good consistency between density profiles and excluded flux measurements at all times. The FRC separatrix slowly shrinks radially because of residual magnetic flux decay.

Such long-lived FRCs could not be obtained without NB injection. Average FRC lifetimes are shown in Fig. 8 as functions of NB duration. The NBs (2.8 MW, 20 keV Hydrogen, 8 ms long pulses) are initiated at $t = -3$ ms (they contribute to preionization before FRC formation) and are stopped at various times (up to $t \sim 5$ ms) during the FRC lifetime. Each trace in Fig. 8 is the midplane excluded flux lifetime averaged over 10 to 20 similar discharges. One observes longer FRC lifetimes with increasing NB durations. The HPF regime corresponds to NB durations greater than 2 to 3 ms. Longer NB durations do not lead to further improvements because of separatrix axial and radial shrinkage. The NB input power to the FRC decreases when separatrix lengths are less than ~2 m and separatrix radii are less than ~0.3 m. All discharges in Fig. 8 are taken with plasma gun and end plugs on, and without quadrupole currents ($q = 0$).

The relative importance of plasma gun, magnetic end plugs, and quadrupoles to the HPF regime is shown in Fig. 9, for similar discharge averages as in Fig. 8. The NB duration is 6 ms ($t \sim -3$ ms to $t \sim 3$ ms) for all data. The error bars are standard deviations for each data set. The HPF regime is obtained with gun and plugs on, and with $q = 0$. Most important is plasma gun operation. Without it, FRC lifetimes are limited to about 1 ms,[3,4] with or without NB injection. Operation with low quadrupole currents ($q < 0.2$) is also important. The FRC lifetimes are reduced significantly for $q = 0.6$, as shown in Fig. 9. For $q = 1$ (not shown), the FRC lifetimes are again limited to ~1 ms.[3,4] Operation with end plugs off shows a modest reduction in FRC lifetimes. Hence, the end plugs have the least importance for the HPF regime.

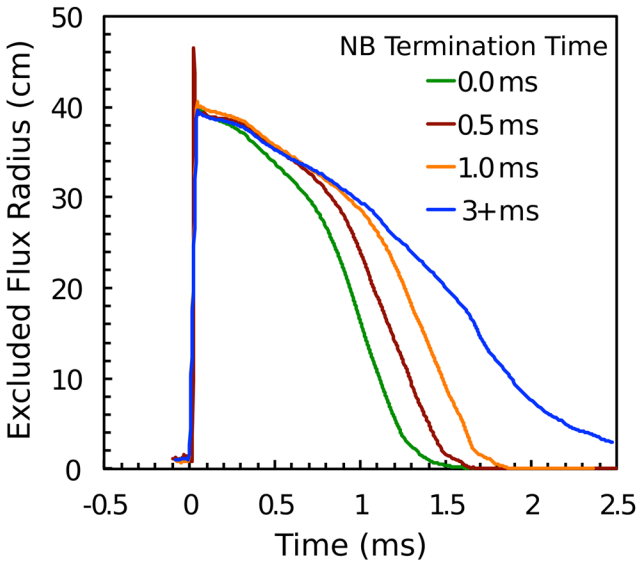

FIG. 8. Excluded flux radii measured as functions of time for various NB durations.

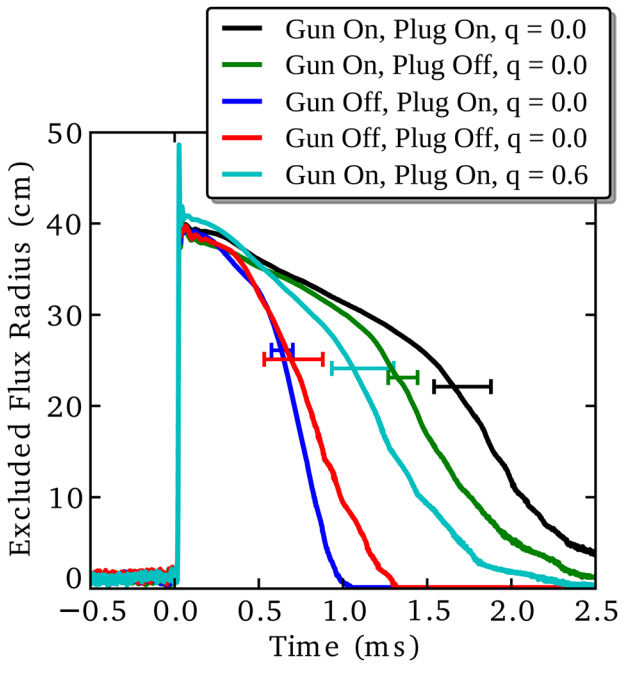

FIG. 9. Excluded flux radii measured as functions of time for various gun, plug, and quadrupole conditions.

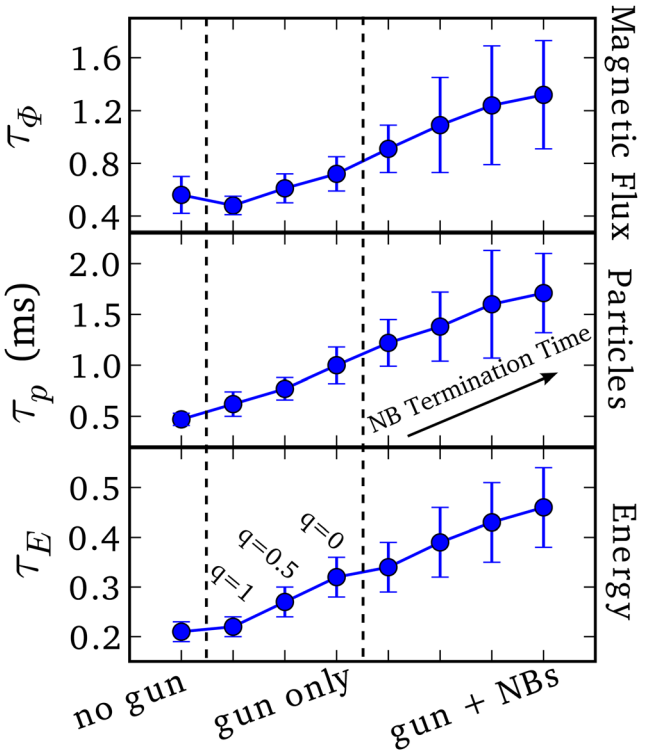

FIG. 10. Average FRC confinement times for various data sets.

The HPF plasma confinement is significantly improved compared to previous FRC data.[3,4] This is illustrated in Fig. 10, with shot-averaged values of e-folding FRC confinement times for (a) magnetic flux, (b) particles, and (c) energy. The standard deviations are included for each data set. All confinement times are determined over the first 0.5 ms. The global energy confinement times are estimated from zero-dimensional, time-dependent, analysis.[17]

The first data set (no gun) includes the best discharges obtained in past C-2 operation.[3,4] The three next data sets (gun only) are obtained with the plasma gun and with the end plugs, without NB injection, and with various quadrupole strengths. The confinement times strongly increase as q decreases from 1 to 0.5 and to 0. Particle transport appears especially improved, compared to magnetic flux confinement. The energy confinement also improves, because convection is a significant contribution.

The last four data sets are obtained with plasma gun and with the end plugs, with $q = 0$ and with NB injection of increasing duration, such as in Fig. 8. The HPF operating regime is obtained with the last two data sets. The HPF particle and magnetic flux confinement times exceed the established FRC scaling from the Large s Experiment (LSX) experiment[18] by factors up to 7.

NB injection yields several other positive results that are currently under detailed investigation. Increased plasma temperatures, increased D-D neutron yields (from $\sim 2 \times 10^5$ to $\sim 10^6$ because of longer FRC lifetimes), and increased $n = 2$ rotational stability are observed. The latter is illustrated in Fig. 11, with ratios of $n = 2$ stable period τ_s (time interval before $n = 2$ onset[1]) to FRC lifetime τ_L as functions of NB duration. Each ratio is the average of 10 to 20 similar discharges, and the standard deviations are included. The ratios cannot exceed unity by definition. Clearly, increased NB duration up to ~ 1 ms improves $n = 2$ stability.

V. DISCUSSION

The AMBAL plasma gun produces an inward radial electric field in the FRC edge layer (Fig. 3) and a good electrical connection through the entire C-2 device (Fig. 4). As a result, the growth of the $n = 2$ rotational mode can be prevented without quadrupole magnetic fields (Fig. 5). The gun operation remains to be explored in more detail. Due to design limitations, the gun electric field could not be increased significantly and could not be reversed. Decreases in gun current and electric field yield shorter-lived FRCs. Gas injection in front of the gun produces cold plasma streams that do not produce HPF results.

The plasma gun drives a somewhat faster $n = 1$ wobble mode in the electron diamagnetic direction (Fig. 6). The $n = 1$ mode amplitude is relatively small, presumably because of partial line-tying to the gun anode. Partial line-tying of the $n = 1$ mode requires sufficiently low sheath resistances.[9,19] Low resistances are achieved in the C-2 device, with sufficiently large gun plasma densities (a few times 10^{18} m^{-3}) relative to FRC edge layer densities ($\sim 10^{19}$ m^{-3}).

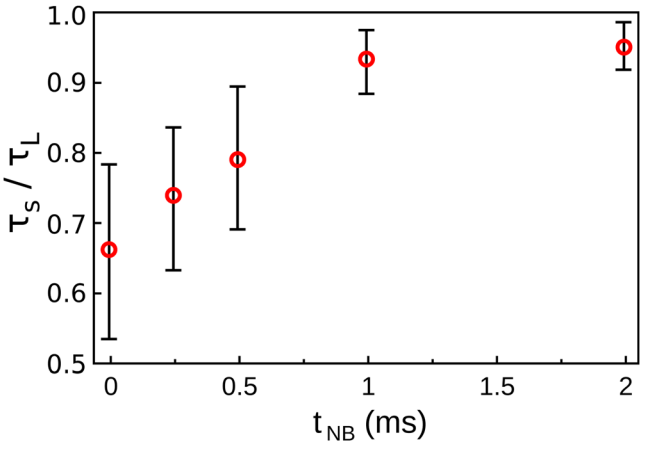

FIG. 11. Average ratios of FRC stable period to FRC lifetime for various NB durations.

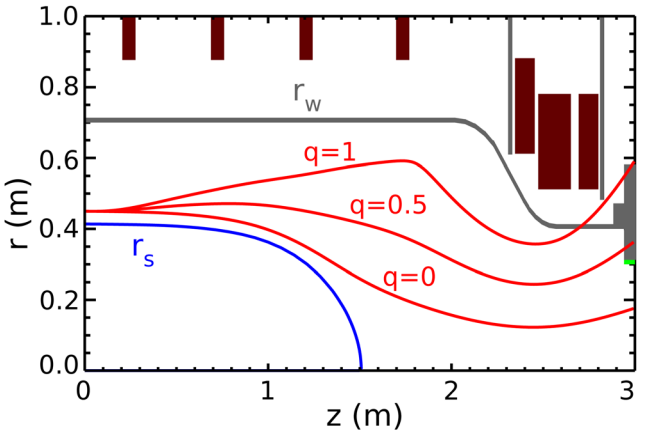

FIG. 12. Calculated edge layer field lines as functions of relative quadrupole current.

The HPF regime requires sufficiently low ($q < 0.2$) quadrupole currents (Fig. 9). The latter are effective in stabilizing the $n = 2$ mode, but they also have negative effects. They compromise the NB fast ion confinement by breaking axisymmetry. They also degrade the FRC edge layer confinement by opening magnetic field lines.[20] This is illustrated in Fig. 12, with C-2 edge layer field lines calculated for different q values, starting at $z = 0$ and $r = 0.45$ m. These Lamy ridge calculations are made in the planes between the quadrupole bars. The open field lines pass through the ends of the confinement vessel for $q = 0$, but they intersect the chamber wall as q increases. This breaks the communication between the FRC and the plasma gun, shorts the gun electric field to the metal wall, and compromises the HPF regime.

The pulsed end magnetic plugs have a relatively little effect on the HPF regime (Fig. 9). This is because the C-2 dc coils (Fig. 1) provide a 2.5 kG magnetic field at the plug locations. This magnetic field is sufficient to transmit $\sim 70\%$ of the edge layer magnetic flux passing through the formation regions. Hence, operating the plugs improves only slightly the connection between the FRC and the end gun. The FRC confinement has a weak or no dependence on the end plug mirror ratio, unlike a mirror confined plasma.

The plasma gun current is turned on after FRC formation and rises in about 0.2 to 0.3 ms. The edge layer starts to rotate in the electron diamagnetic direction, while the FRC rotates in the opposite direction. Hence, there probably is $E \times B$ velocity shear near the FRC separatrix. Velocity shear has been shown to reduce turbulent transport and convection in many plasmas.[21] Similar physics may occur for C-2 FRCs operated with the plasma gun.

The FRC particle confinement times are calculated neglecting all particle sources (Fig. 10). The gun plasma, NBs, and neutrals are small sources compared to the FRC particle decay rates. The gun plasma line-integrated densities (measured with 140 GHz microwave interferometry in the confinement vessel) are only a few percent of the FRC line-integrated densities. In addition, the gun plasma presumably flows in the edge layer rather than inside the FRC. The NBs (<250 A) are a negligible particle source. Recycling and neutral ionization inside the FRC are also inferred to be small sources, by comparing FRC data sets taken under similar conditions, but with and without wall gettering.[22] The average particle confinement times are found similar, within experimental uncertainties.

The FRC confinement in the HPF regime further improves with NB injection (Fig. 10). While the NBs appear to maintain the FRC diamagnetism, the apparent increases in magnetic flux confinement time require further analysis to separate possible contributions from heating and current drive. The NB fast ions slow down primarily through electron collisions. The latter occur in the edge layer as well as inside the FRC. The respective contributions of both regions need to be clarified with additional data and calculations. HPF studies with NB beam powers other than 2.8 MW and with other beam energies remain to be done.

The $n = 2$ rotational mode appears to be further stabilized by NB fast ions. The $n = 2$ mode stabilization increases with NB durations up to ~ 1 ms and is nearly complete for longer durations (Fig. 11). A stabilizing effect from NB fast ions has been found in past theoretical analysis.[23] However, more complete calculations, including kinetic effects and arbitrary rotation profiles, are required to support these observations and to clarify the physics of the HPF operating regime. The HPF operating regime may well have limits, since rotational modes can develop for both signs of the azimuthal rotation.[24]

The end plasma gun is the most successful method of radial electric field control attempted so far in the C-2 device. This is presumably because the FRC separatrix connects to the geometrical axis, so that electrical biasing near $r = 0$ has the greatest influence on the FRC. Partial success was obtained by biasing positively ring electrodes that connect to field lines in between the FRC and the wall.[22] Such biasing produced an inward electric field, some $n = 2$ rotational stabilization, but no HPF data. Electrical bias applied to a set of concentric electrodes at $z = 10$ m (Fig. 1) proved ineffective, probably because quadrupoles were used ($q = 1$) and because low divertor magnetic fields (plasma densities) compromised partial line-tying to the electrodes.

VI. SUMMARY

A plasma gun, placed at one end of the C-2 device, yields an inward radial electric field in the FRC edge layer. This counters the usual FRC spin-up. As a result, the dangerous $n = 2$ rotational instability is controlled without applying quadrupole magnetic fields. Better plasma centering is also obtained, presumably from line-tying to the gun electrodes. The FRC discharges are nearly axisymmetric, which improves NB fast ion confinement. The combined effects of the plasma gun and of NB injection lead to the HPF operating regime. HPF data show FRC lifetimes up to 3 ms, and FRC confinement times improved by factors 2 to 4.

The HPF operating regime described in the present paper yields much of the improvements in plasma stability and confinement that are required before attempting FRC sustainment in the C-2 device. In the middle of the FRC lifetime (~ 1 ms), the FRC global power losses are ~ 4 MW for HPF discharges, which is within reach of the available injected NB power. FRC sustainment may be possible in near-term experiments, with increased NB power and pellet refueling.

ACKNOWLEDGEMENTS

We thank our shareholders for their support and trust and the rest of the TAE staff for their dedicated, excellent work. We are especially thankful to many members of the Budker Institute for technical excellence and for consistently superb on-site assistance with the NBs and the plasma gun.

[1]M. Tuszewski, Nucl. Fusion **28**, 2033 (1988).
[2]L. C. Steinhauer, Phys. Plasmas **18**, 070501 (2011).
[3]M. W. Binderbauer, H. Y. Guo, M. Tuszewski, S. Putvinski, L. Sevier, D. Barnes, N. Rostoker, M. G. Anderson, R. Andow, L. Bonelli, F. Brandi, R.

Brown, D. Q. Bui, V. Bystritskii, F. Ceccherini, R. Clary, A. H. Cheung, K. D. Conroy, B. H. Deng, S. A. Dettrick, J. D. Douglass, P. Feng, L. Galeotti, E. Garate, F. Giammanco, F. J. Glass, O. Gornostaeva, H. Gota, D. Gupta, S. Gupta, J. S. Kinley, K. Knapp, S. Korepanov, M. Hollins, I. Isakov, V. A. Jose, X. L. Li, Y. Luo, P. Marsili, R. Mendoza, M. Meekins, Y. Mok, A. Necas, E. Paganini, F. Pegoraro, R. Pousa-Hijos, S. Primavera, E. Ruskov, A. Qerushi, L. Schmitz, J. H. Schroeder, A. Sibley, A. Smirnov, Y. Song, X. Sun, M. C. Thompson, A. D. Van Drie, J. K. Walters, M. D. Wyman, and the TAE Team, Phys. Rev. Lett. **105**, 045003 (2010).

[4]H. Y. Guo, M. W. Binderbauer, D. Barnes, S. Putvinski, N. Rostoker, L. Sevier, M. Tuszewski, M. G. Anderson, R. Andow, L. Bonelli, F. Brandi, R. Brown, D. Q. Bui, V. Bystritskii, F. Ceccherini, R. Clary, A. H. Cheung, K. D. Conroy, B. H. Deng, S. A. Dettrick, J. D. Douglass, P. Feng, L. Galeotti, E. Garate, F. Giammanco, F. J. Glass, O. Gornostaeva, H. Gota, D. Gupta, S. Gupta, J. S. Kinley, K. Knapp, S. Korepanov, M. Hollins, I. Isakov, V. A. Jose, X. L. Li, Y. Luo, P. Marsili, R. Mendoza, M. Meekins, Y. Mok, A. Necas, E. Paganini, F. Pegoraro, R. Pousa-Hijos, S. Primavera, E. Ruskov, A. Qerushi, L. Schmitz, J. H. Schroeder, A. Sibley, A. Smirnov, Y. Song, L. C. Steinhauer, X. Sun, M. C. Thompson, A. D. Van Drie, J. K. Walters, M. D. Wyman, and TAE Team, Phys. Plasmas **18**, 056110 (2011).

[5]L. Galeotti, D. C. Barnes, F. Ceccherini, and F. Pegoraro, Phys. Plasmas **18**, 082509 (2011).

[6]M. Tuszewski, G. A. Barnes, R. E. Chrien, W. N. Hugrass, D. J. Rej, R. E. Siemon, and B. Wright, Phys. Fluids **31**, 946 (1988).

[7]M. Tuszewski, G. A. Barnes, M. H. Baron, R. E. Chrien, W. N. Hugrass, P. L. Klingner, C. Ng, D. J. Rej, D. P. Taggart, R. E. Siemon, and B. Wright, Phys. Fluids B **2**, 2541 (1990).

[8]S. Ohi, T. Minato, Y. Kawakami, M. Tanjyo, S. Okada, Y. Ito, M. Kako, S. Goto, T. Ishimura, and H. Ito, Phys. Rev. Lett. **51**, 1042 (1983).

[9]D. Ryutov, H. L. Berk, B. I. Cohen, A. W. Molvik, and T. C. Simonen, Phys. Plasmas **18**, 092301 (2011).

[10]J. M. Finn, Plasma Phys. **21**, 405 (1979).

[11]R. H. Cohen, D. V. Anderson, and C. B. Sharp, Phys. Rev. Lett. **41**, 1304 (1978).

[12]A. F. Lifschitz, R. Farengo, and A. L. Hoffman, Nucl. Fusion **44**, 1015 (2004).

[13]G. I. Dimov, A. A. Ivanov, and G. V. Roslyakov, Sov. J. Plasma Phys. **8**, 546 (1982).

[14]T. D. Akhmetov, V. S. Belkin, I. O. Bespamyatnov, V. I. Davydenko, G. I. Dimov, Yu. V. Kovalenko, A. S. Krivenko, P. A. Potashov, V. V. Razorenov, V. B. Reva, V. Ya. Savkin, and G. I. Shulzhenko, Trans. Fusion Sci. Technol. **43**, 58 (2003).

[15]O. Gornostaeva, B. H. Deng, E. Garate, H. Gota, J. Kinley, J. Schroeder, and M. Tuszewski, Rev. Sci. Instrum. **81**, 10D516 (2010).

[16]M. Tuszewski, Plasma Phys. Controlled Fusion **26**, 991 (1984).

[17]D. J. Rej and M. Tuszewski, Phys. Fluids **27**, 1514 (1984).

[18]A. L. Hoffman and J. T. Slough, Nucl. Fusion **33**, 27 (1993).

[19]A. W. Molvik, R. A. Breun, S. N. Golovato, N. Hershkowitz, B. McVey, R. S. Post, D. Smatlak, and L. Yujiri, Phys. Fluids **27**, 2711 (1984).

[20]J. H. Hammer and H. L. Berk, Nucl. Fusion **22**, 89 (1982).

[21]K. H. Burrell, Phys. Plasmas **4**, 1499 (1997).

[22]H. Gota, M. W. Binderbauer, H. Y. Guo, M. Tuszewski, D. Barnes, L. Sevier, N. Rostoker, R. Brown, D. Q. Bui, F. Ceccherini, R. Clary, K. D. Conroy, B. H. Deng, S. A. Dettrick, J. D. Douglass, L. Galeotti, E. Garate, F. J. Glass, D. Gupta, S. Gupta, J. S. Kinley, K. Knapp, S. Korepanov, M. Hollins, X. L. Li, Y. Luo, R. Mendoza, Y. Mok, A. Necas, S. Primavera, E. Ruskov, L. Schmitz, J. H. Schroeder, A. Sibley, A. Smirnov, Y. Song, X. Sun, M. C. Thompson, E. Trask, A. D. Van Drie, J. K. Walters, M. D. Wyman, and the TAE Team, in *Proceedings of the 2011 ICC Workshop, Seattle* [J. Fusion Energy (2012)] (to be published).

[23]M. Ohnishi, H. Kuranaga, and M. Okamoto, Nucl. Fusion **28**, 1427 (1988).

[24]J. P Freidberg and L. D. Pearlstein, Phys. Fluids **21**, 1207 (1978).